A current controller of grid-connected converter for harmonic damping in a distribution network

Wang, Xiongfei; Blaabjerg, Frede; Chen, Zhe

Published in:
Proceedings of the International Conference on Electrical Machines and Systems, ICEMS 2011

DOI (link to publication from Publisher):
10.1109/ICEMS.2011.6073975

Publication date:
2011

Document Version
Early version, also known as pre-print

A Current Controller of Grid-Connected Converter for Harmonic Damping in a Distribution Network

Xiongfei Wang, Frede Blaabjerg, Zhe Chen
Department of Energy Technology, Aalborg University, Denmark
E-mail: xwa@et.aau.dk, fbl@et.aau.dk, zch@et.aau.dk

Abstract — Harmonic resonance caused by the increased use of shunt-connected capacitors in LCL-filters and power factor correction devices may become a serious power quality challenge in electric distribution systems. A voltage-detection method based on current control is developed to damp harmonic resonances. However, it is susceptible to the mismatch between harmonic conductance and characteristic impedance of distribution feeder. This paper proposes a current controller which allows discrete adjustment of harmonic conductance for both the characteristic harmonic and the non-characteristic harmonic voltages. Thus, the unintentional impedance mismatch can be attenuated to a large extent, and a lower power rating compared to the conventional control method is maintained. Simulations and laboratory tests are performed to verify the overall performance of the proposed controller.

I. Introduction

Switch-mode power converters are gaining wide acceptance to provide efficient and flexible interfaces for both distributed generation (DG) units and various electric loads thanks to the emerging power electronics technology [1]. On the other hand, harmonic pollution which stems from nonlinear electronic devices may deteriorate the power quality of the distribution systems [2]. Moreover, with the increased use of LCL-filters for grid-connected converters, the harmonic resonances caused by the aggregated shunt-connected capacitors in the LCL-filters, capacitive loads, and power factor correction (PFC) capacitors are also becoming a power quality challenge [3].

An active harmonic filtering function is deemed to be one of ancillary services provided by grid-connected converters, such as PWM rectifier and inverter-interfaced DG units [2]. A number of current control methods are available for grid-connected converters with an active filtering function, but few of them can be used to mitigate harmonic interactions between grid-connected converters, and to damp the resultant harmonic resonance [5]. Recently, voltage-detection method based on current control was implemented in grid-connected converters for harmonic damping in a distribution system [6]-[8]. Instead of preserving sinusoidal current, a distorted current of which the harmonic components are in phase with the output voltage of the converter is produced by the grid-connected converter. As a consequence, the converter operates like a resistor at the harmonic frequency, thus the harmonic resonance throughout a distribution feeder can be damped [6]. However, the performance of this approach is degraded in the case of the mismatch between the harmonic conductance and the characteristic impedance of distribution feeder [7]. The harmonic voltage of a certain bus is magnified even though the harmonic voltage at the output of the converter is suppressed. This phenomenon is also named as 'whack-a-mole' effect [8]. Furthermore, a higher power rating of the converter is required since it is based on global harmonic voltage detection [9]. To avoid the unintentional 'whack-a-mole' problem, a discrete harmonic conductance adjustment scheme was proposed based on the selective harmonic voltage detection [10]. But it is assumed that harmonic resonances only arise at the characteristic harmonic frequencies, whereas the non-characteristic harmonic resonance damping was not taken into account. It has been shown that the even (4^{th}) harmonic resonance problem arises in an electrochemical plant in [11].

This paper proposes a current controller for grid-connected converter which can suppress the non-characteristic harmonic resonance, and simultaneously maintain a lower power rating of converter compared to the conventional global harmonic voltage detection based method. In the approach, an automatic tuning conductance is synthesized for the non-characteristic harmonic voltage in addition to the characteristic harmonic conductance loops. Thus, the unintentional 'whack-a-mole' problem can be significantly attenuated even in the presence of the non-characteristic harmonic resonance. Simulations and laboratory test results are presented to verify the performance of the current controller.

II. Operation Principle

Fig. 1 illustrates a simplified model of a distribution system and the proposed current controller. The voltage-source converter is connected to the distribution system through an LCL filter of which the capacitor voltage is decomposed to synthesize the harmonic conductance at both the characteristic and the non-characteristic harmonic frequencies. The even harmonic voltages are assumed to be present in the grid, so as to emulate the unusual non-characteristic harmonic resonance problem [11]. A three-phase diode rectifier load is connected to the Point of Common Coupling (PCC) of the converter.

Based on the voltage detection, the current reference can be derived as

$$\begin{pmatrix} i_\alpha^* \\ i_\beta^* \end{pmatrix} = G_f^* V_{\alpha\beta f} + \begin{pmatrix} G_5^* & \cdots & 0 \\ \vdots & \ddots & \vdots \\ 0 & \cdots & G_h^* \end{pmatrix} \begin{pmatrix} V_{\alpha\beta 5} \\ \vdots \\ V_{\alpha\beta h} \end{pmatrix} + G_{nch}^* V_{\alpha\beta nch} \qquad (1)$$

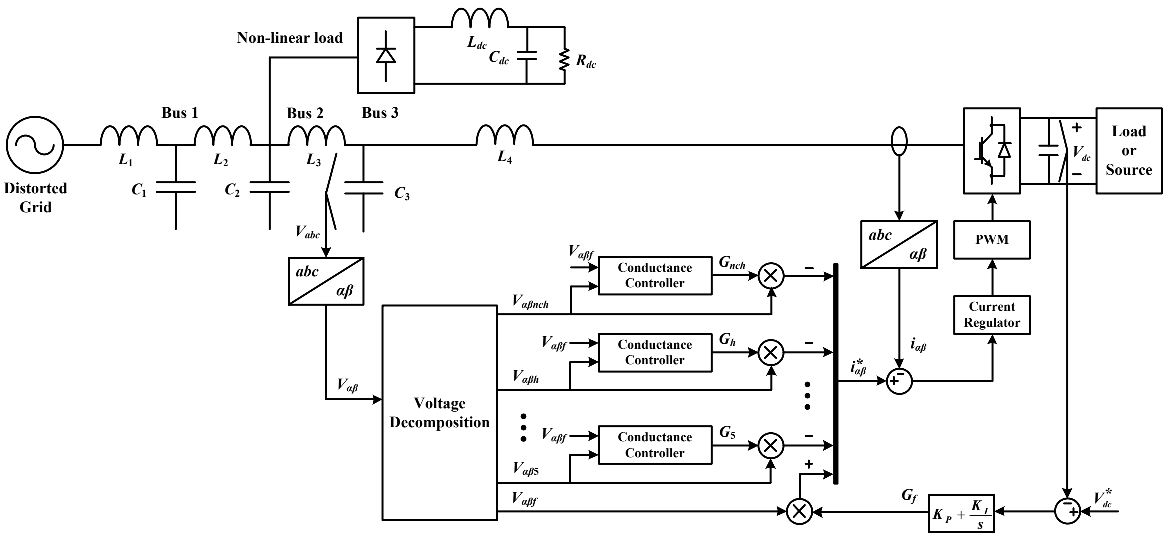

Fig. 1. A simple model of distribution system and the proposed current controller.

where the fundamental conductance G_f is used to regulate the output active power, and a bidirectional operation with unity power factor is therefore achieved by multiplying the G_f with the fundamental frequency voltage $V_{\alpha\beta f}$. The $G_5 \ldots G_h$ are the characteristic harmonic conductance, which are adjusted based on the distortion limits of characteristic harmonic voltages, $V_{\alpha\beta f}$, $V_{\alpha\beta 5} \ldots V_{\alpha\beta h}$. The non-characteristic harmonic conductance G_{nch} is regulated considering the limit of the non-characteristic harmonic voltage $V_{\alpha\beta nch}$.

A. Output Voltage Decomposition

Fig. 2 shows a block diagram of the voltage decomposition algorithm based on the multiple reference frame theory [12]. The Second Order Generalized Integrator (SOGI) based Phase-Locked Loop (PLL) topology is adopted to synchronize with the grid [13]. The characteristic harmonic voltages are transformed into dc constants in each rotating frame. A low-pass filter with 10 Hz cutoff frequency is used to decouple the interactions between different reference frames. On the other hand, the non-characteristic harmonic voltage $V_{\alpha\beta nch}$ is derived by subtracting the sum of the fundamental frequency voltage and the characteristic voltages from the output voltage $V_{\alpha\beta}$.

B. Harmonic Conductance Controller

The harmonic resonance frequency of a distribution feeder is usually susceptible to the variations of circuit parameters, such as the changes of shunt-connected capacitors, different operation modes of grid-connected converters, and various load conditions. Hence, it is important to regulate adaptively the harmonic conductance based on the allowed harmonic voltage distortion limits. There are two schemes for automatic adjustment of the harmonic conductance [14], [7]. The first scheme consists of a sign detector and a step up-down counter to adjust the harmonic conductance [14]. The second one is the proportional-integral (PI) based controller that is adopted in this work [7].

Fig. 3 shows a block diagram of the harmonic conductance controller. The low-pass filters with 10 Hz cutoff frequency and square operations can be used to approximately calculate

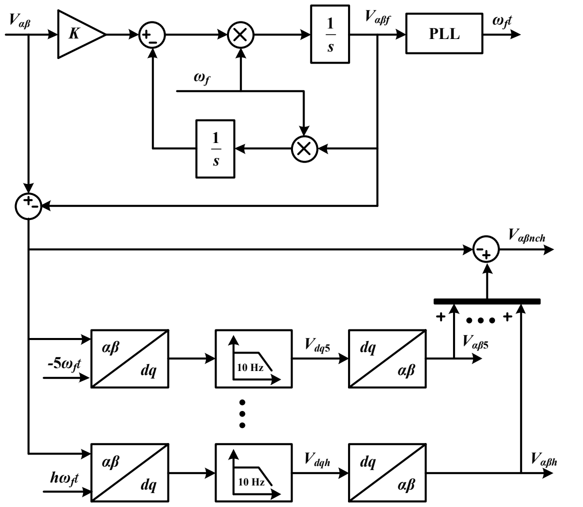

Fig. 2. Block diagram of output voltage decomposition algorithm based on the multiple reference frame theory.

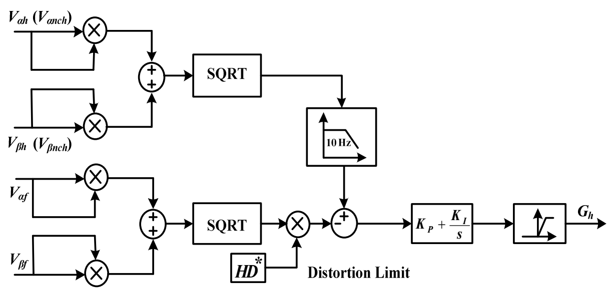

Fig. 3. Block diagram of the harmonic conductance controller.

the rms value of the harmonic voltage distortion [7].

$$|V_h| = \sqrt{V_{\alpha h}^2 + V_{\beta h}^2} \tag{2}$$

$$|V_{nch}| = \sqrt{V_{\alpha nch}^2 + V_{\beta nch}^2} \quad (3)$$

It is worth to note that the dynamic performance of the non-characteristic harmonic conductance loop is influenced by the characteristic harmonic conductance. This is due to the use of negative feedback loops in the derivation of non-characteristic harmonic voltage. A higher proportional or integral term in the PI controller of non-characteristic impedance loop may lead to oscillations of characteristic harmonic conductance. However, a compromise can be found in tuning of PI controllers, due to the slow variation of the harmonic voltage [14].

III. SIMULATION RESULTS

A 6.2 kVA 400 V three-phase distribution system which is shown in Fig. 1 is tested in both simulations and laboratory tests to evaluate the performance of the proposed current controller. The main parameters of the system are shown in Table I. Due to the presence of non-characteristic resonance at the even harmonic frequencies, the 4th (2%) and 6th (1%) harmonic voltages are assumed to be present in grid voltage, the harmonic spectrum of which is shown in Fig. 4. The grid-connected converter operates as a PWM rectifier (unity power factor) with 3.2 kW dc load.

Fig. 5 (a) shows the per-phase bus voltages without using any harmonic damping control, and a sinusoidal input current is produced in the PWM rectifier. It is observed that the bus voltages are severely distorted. Fig. 6 (a) shows the harmonic spectrums of the bus voltages. It can be seen that the harmonic resonance arises at the 4th harmonic frequency. Moreover, the unintentional 2nd, 10th, 14th and 16th harmonic voltages also appear along the distribution feeder.

Fig. 5 (b) shows the per-phase bus voltages under the use of the discrete-frequency tuning harmonic damping control in [7]. Since only the characteristic harmonic voltage is of concern in this method, the even harmonic resonance cannot be damped. The bus voltage distortions are still high. Fig. 6 (b) shows the related harmonic spectrums. Compared with Fig. 6 (a), it can be observed that the characteristic harmonic voltages are well damped, but the 4th harmonic resonance becomes more severe unfortunately. It implies that the diode rectifier has a damping effect on 4th harmonic resonance in this case. Similar results can be found in laboratory tests, as shown in Fig. 9 and Fig. 10.

TABLE I
MAIN PARAMETERS OF THE DISTRIBUTION SYSTEM

Line inductor	L_1	3.5 mH
	L_2=L_3	3 mH
	L_4	1.5 mH
Shunt-connected capacitor	C_1	100 μF
	C_2	50 μF
	C_3	25 μF
Diode rectifier	L_{dc}	84 μH
	C_{dc}	235μF
	R_{dc}	550 Ω
PWM rectifier	V_{dc}	750 V

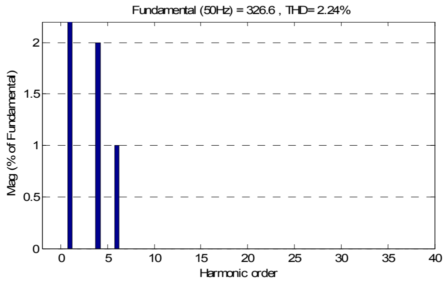

Fig. 4. The harmonic spectrum of simulated grid voltage.

Fig. 5 (c) shows the per-phase bus voltage waveforms with the proposed current control method, and the related harmonic spectrums are given in Fig. 6 (c). It is clear that the voltage distortions are reduced significantly. The 4th harmonic voltage resonance and other unintentional non-characteristic harmonic voltages are effectively damped.

IV. EXPERIMENTAL RESULTS

To evaluate the performance of the current controller under different load conditions, the light load and heavy load cases

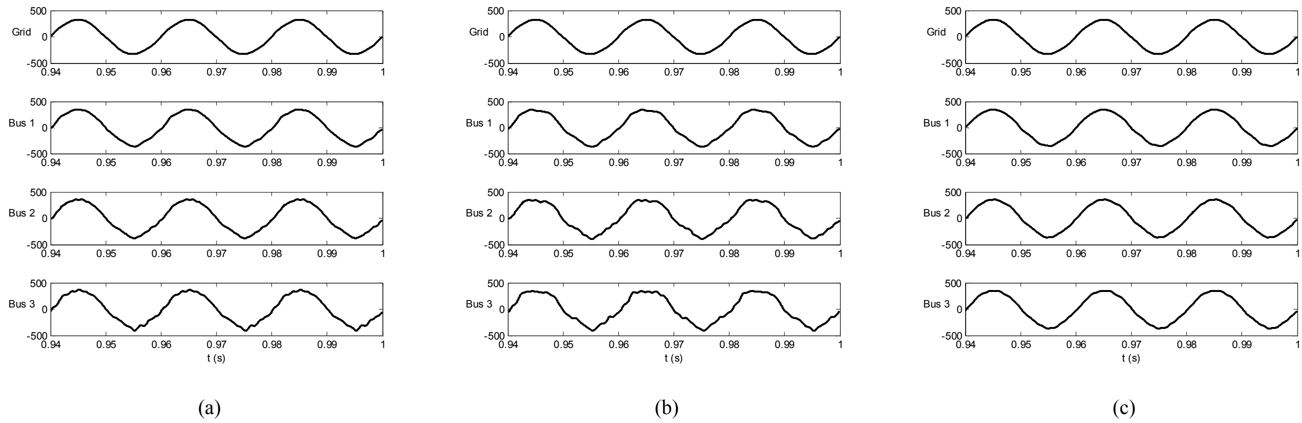

Fig. 5. Simulated bus voltages with three different control methods. (a) Without any harmonic damping control. (b) With discrete-frequency tuning control [7]. (c) With the proposed current control.

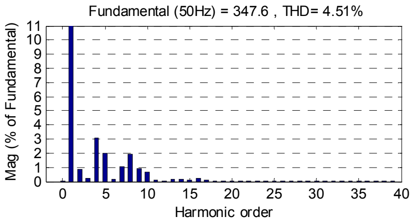

(a-1) Bus 1

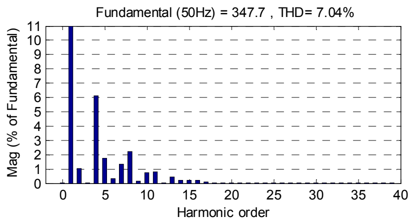

(b-1) Bus 1

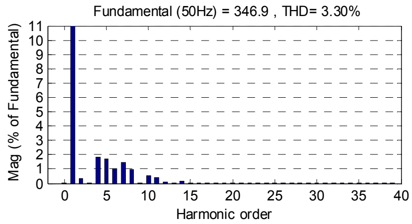

(c-1) Bus 1

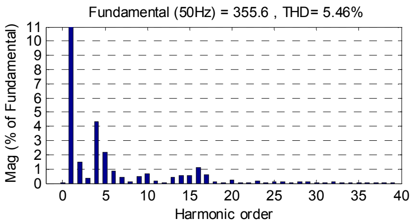

(a-2) Bus 2

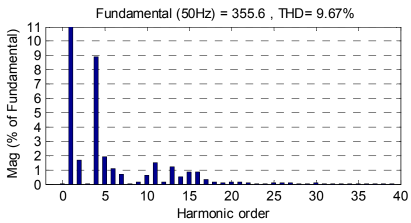

(b-2) Bus 2

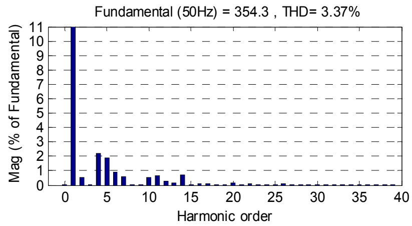

(c-2) Bus 2

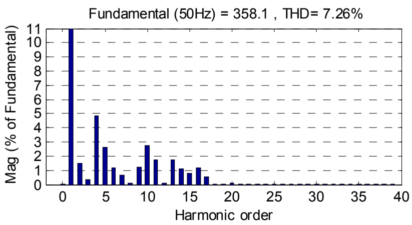

(a-3) Bus 3

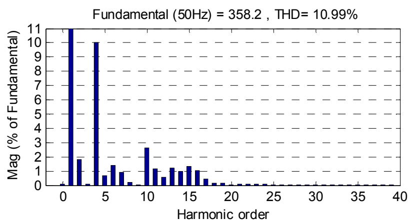

(b-3) Bus 3

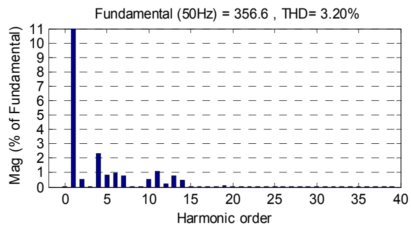

(c-3) Bus 3

Fig. 6. Harmonic spectrum analysis of simulated bus voltages with three different control methods. (a) Without any harmonic damping control. (b) With discrete-frequency tuning control [7]. (c) With the proposed current control.

are tested on the laboratory setup, respectively. Table II gives the load conditions, where the heavy load parameters are the same as the load parameters used in the simulations. A 6.2 kVA laboratory grid simulator is utilized to generate the needed 4th and 6th harmonic voltages. Fig. 7 shows the measured voltage waveform of the grid simulator and the related harmonic spectrum. The proposed current controller is implemented in the DS1006 dSPACE system using 10 kHz sampling frequency. A 5 kW Danfoss converter is controlled to operate as a PWM rectifier.

Similar to simulations, the voltage distortions with the three different current control methods are tested on the laboratory setup, respectively. Fig. 8 shows the per-phase bus voltages measured in heavy load (0.6 pu) condition. The corresponding harmonic spectrum for the terminal voltage of converter (bus 3) is shown in Fig. 9. It can be observed that the 4th harmonic resonance arises in the experiment, which is the same as in simulations. Since the equivalent series resistances (ESR) of the LC components are much higher in practical applications, a lower 4th harmonic voltage is observed in the experiments.

Also, it is noted that the unintentional non-characteristic 2nd and 10th harmonic voltages appear along the distribution line, as shown in Fig. 9 (a). Similarly, the increase of 4th harmonic voltage and other non-characteristic harmonic voltages can be observed when only applying the discrete-frequency tuning control, as shown in Fig. 9 (b).

Fig. 10 shows the harmonic spectrum analysis result for the terminal voltage of converter (bus 3) under light load (0.1 pu) condition. Note that a more severe harmonic resonance arises

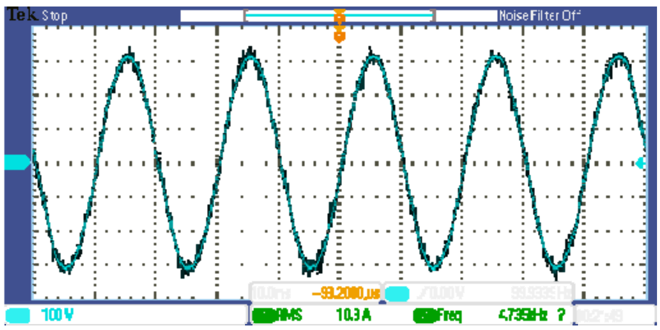

(a)

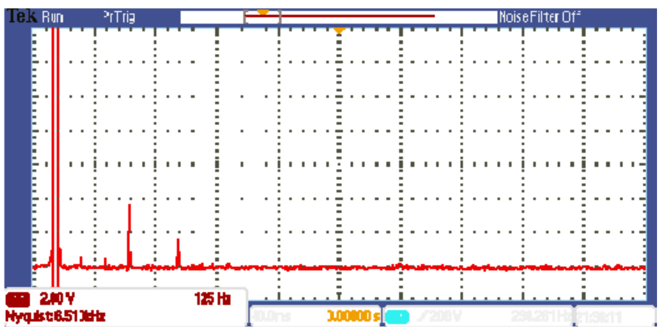

(b)

Fig. 7. The measured grid voltage waveform (100 V/div, 10 ms/div) and the related harmonic spectrum (2 V/div).

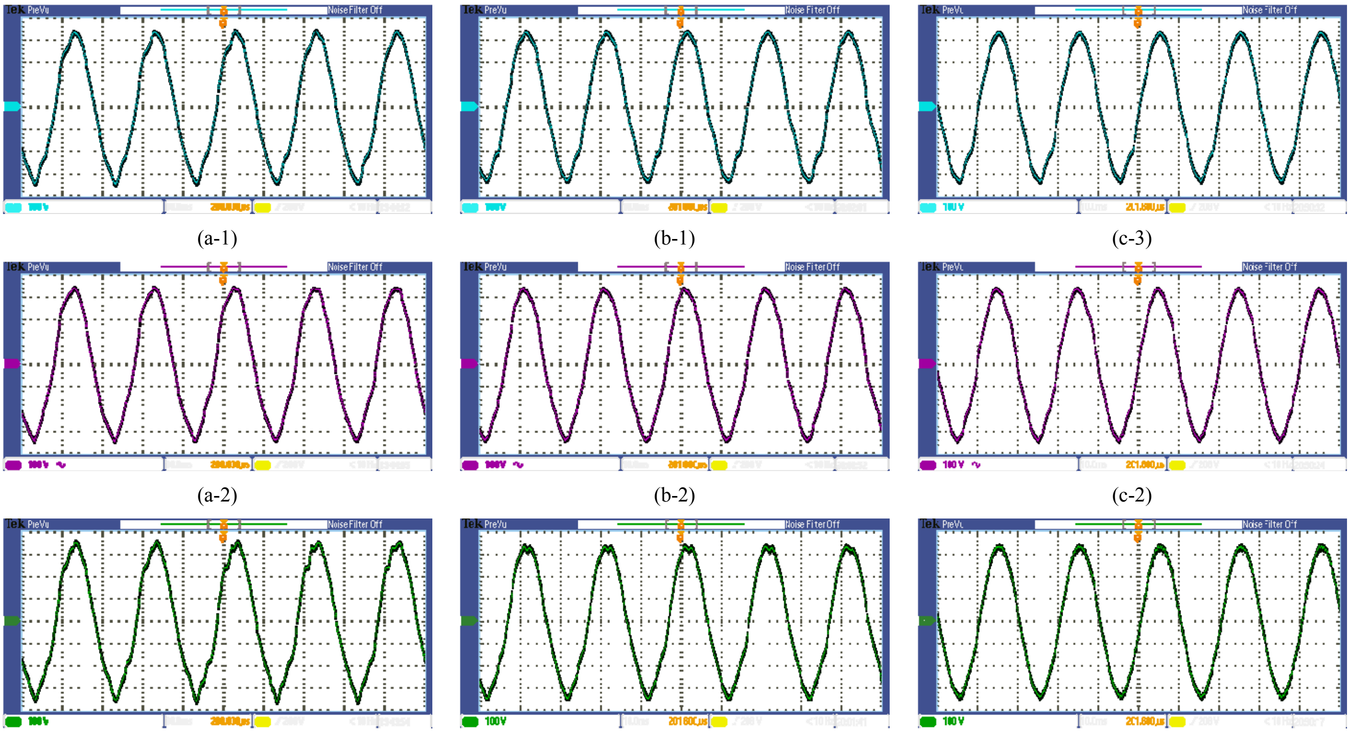

(a-1) (b-1) (c-3)

(a-2) (b-2) (c-2)

(a-3) (b-3) (c-3)

Fig. 8. Measured bus voltages with three different control methods under the heavy load condition (100 V/div, 10 ms/div). (a) Without any harmonic damping control. (b) With discrete-frequency tuning control [7]. (c) With the proposed current control.

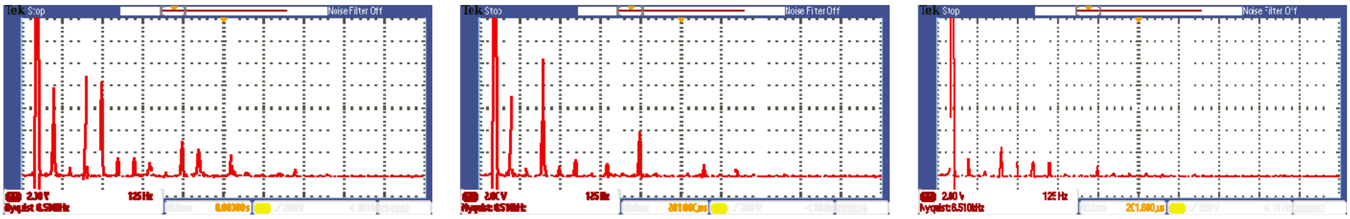

(a) THD (6.84%) (b) THD (5.98%) (c) THD (2.24%)

Fig. 9. Harmonic spectrum analysis of the measured voltage at the terminal of converter (bus 3) under the heavy load condition (2 V/div, 125 Hz/div). ((a) Without any harmonic damping control. (b) With discrete-frequency tuning control [7]. (c) With the proposed current control.

(a) THD (7.19%) (b) THD (5.88%) (c) THD (2.48%)

Fig. 10. Harmonic spectrum analysis of the measured voltage at the terminal of converter (bus 3) under the light load condition (2 V/div, 125 Hz/div). (a) Without any harmonic damping control. (b) With discrete-frequency tuning control [7]. (c) With the proposed current control.

under the light load condition compared to the Fig. 9. Fig. 11 shows the per-phase bus voltages under the light load condition. Also, the voltage distortions are more serious than the heavy load condition. Additionally, it is interesting to note that the 2^{nd} harmonic voltage is not as high as the heavy load case, whereas the 4^{th} harmonic resonance is much more severe. This implies that different load situations may result in various

TABLE II
TWO DIFFERENT LOAD CONDITIONS FOR TEST

Heavy load	Diode rectifier	0.5 kW (0.08 pu)
	PWM rectifier	3.2 kW (0.52 pu)
Light load	Diode rectifier	0.2 kW (0.03 pu)
	PWM rectifier	0.5 kW (0.07 pu)

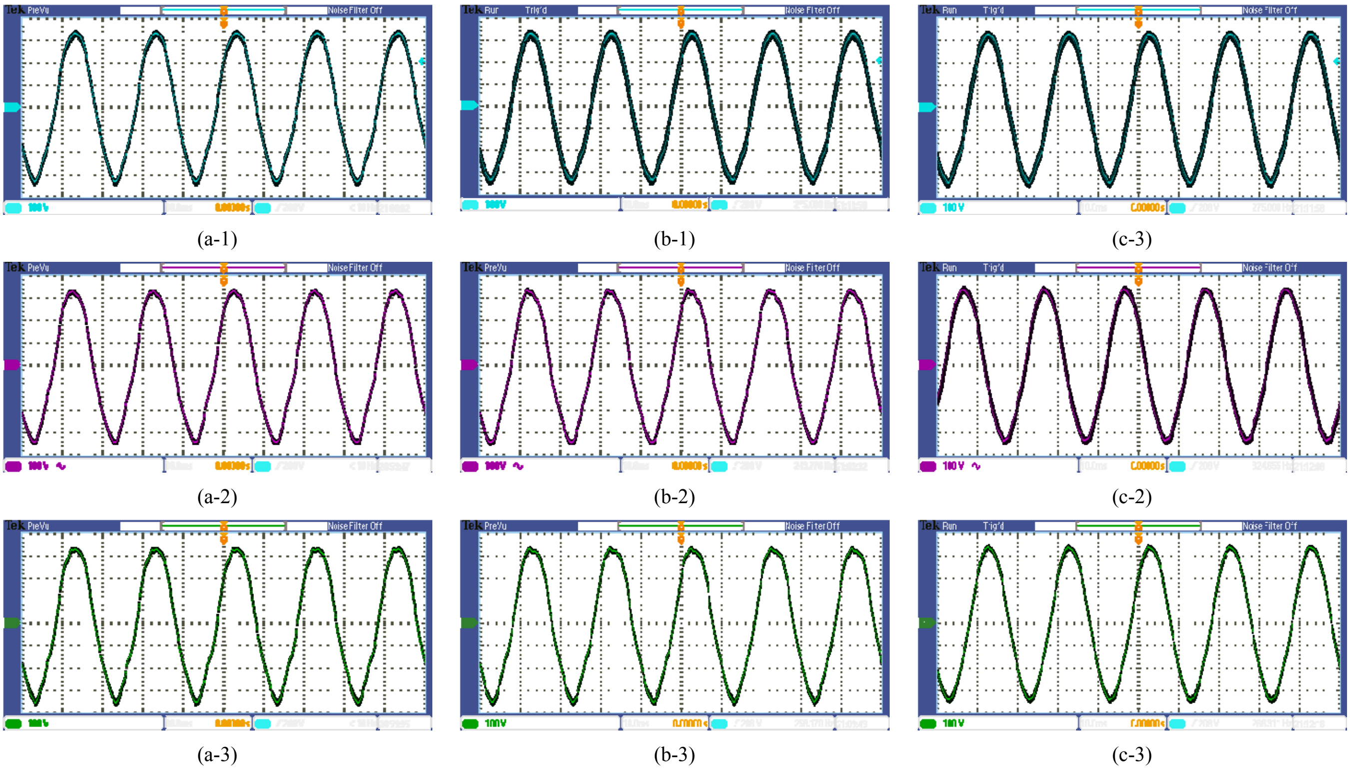

Fig. 11. Measured bus voltages with three different control methods under the light load condition (100 V/div, 10 ms/div). (a) Without any harmonic damping control. (b) With discrete-frequency tuning control [7]. (c) With the proposed current control.

unintentional non-characteristic harmonic voltage distortions. Therefore, the automatic adjustment of harmonic conductance is important to achieve an optimum harmonic damping performance.

V. Conclusions

This paper has discussed a current control method of grid-connected converter for providing harmonic damping function in a distribution system. It can not only damp the characteristic harmonic voltage distortions by separately adjusted harmonic conductance loops, but it can also damp the non-characteristic harmonic resonance through an automatic-tuned conductance loop. Therefore, the unintentional 'whack-a-mole' effect can be attenuated. Simulation and experimental results validated the performance of the current controller.

References

[1] F. Blaabjerg, Z. Chen, and S. B. Kjaer, "Power electronics as efficient interface in dispersed power generation systems," *IEEE Trans. Power Electron*., vol. 19, no. 5, pp. 1184-1194, Sept., 2004.

[2] F. Wang, J. Duarte, M. Hendrix, and P. Ribeiro, "Modelling and analysis of grid harmonic distortion impact of aggregated DG inverters," *IEEE Trans. Power Electron*., vol. 26, no. 3, pp. 786-797, Mar. 2011.

[3] J. H. Enslin and P. J. Heskes, "Harmonic interaction between a large number of distributed power inverters and the distribution network," *IEEE Trans. Power Electron.,* vol. 19, no. 6, pp. 1586-1593, Nov. 2004.

[4] G. Joos, B. T. Ooi, D. McGillis, F. D. Galiana, and R. Marceau, "The potential of distributed generation to provide ancillary services," in *Proc. IEEE PESGM* 2000, pp. 1762-1767.

[5] X. Wang, J. M. Guerrero, Z. Chen, and F. Blaabjerg, "Distributed energy resources in grid interactive AC microgrids," *in Proc. IEEE PEDG* 2010, pp. 806-812.

[6] T. Takeshita and N. Matsui, "Current waveform control of PWM converter system for harmonic suppression on distribution system," *IEEE Trans. on Ind. Electron.*, vol. 50, no. 6, pp. 1134-1139, December 2003.

[7] B. Renders, K. De Guseeme, W. R. Ryckaret and L. Vandevelde, "Input impedance of grid-connected converters with programmable harmonic resistance," *IET Electr. Power Appl.*, vol. 1, no. 3, pp. 355-361, May 2007.

[8] K. Wada, H. Fujita, and H. Akagi, "Considerations of a shunt active filter based on voltage detection for installation on a long distribution feeder," *IEEE Trans. Ind. Applicat.*, vol. 38, pp. 1123-1130, Jul./Aug. 2002.

[9] L. Asiminoaei, F. Blaabjerg, and S. Hansen, "Detection is key-harmonic detection methods for active filter applications," *IEEE Ind. Applicat. Mag.*, vol. 13, no. 4, pp. 22-33, Jul./Aug. 2007.

[10] T. Lee, J. Li, and P. Cheng, "Discrete frequency tuning active filter for power system harmonics," *IEEE Trans. on Power Electron..*, vol. 24, no. 5, pp. 1209-1217, May 2009.

[11] P. C. Buddingh, "Even harmonic resonance-an unusual problem," *IEEE Trans. Ind. Applicat.*, vol. 39, no. 4, pp. 1181-1186, Jul./Aug. 2003.

[12] P. Xiao, K. A. Corzine, and G. K. Venayagamoorthy, "Multiple reference frame-based control of three-phase PWM boost rectifiers under unbalanced and distorted input conditions," *IEEE Trans. on Power Electron..*, vol. 23, no. 4, pp. 2006-2016, Jul. 2008.

[13] M. Ciobotaru, R. Teodorescu and F. Blaabjerg, "A new single-phase PLL structure based on second order generalized integrator," in *Proc. IEEE PESC* 2006, pp. 1-6.

[14] P. Jintakosonwit, H. Akagi, H. Fujita, and S. Ogasawara, "Implementation and performance of automatic gain adjustment in a shunt active filter for harmonic damping throughout a power distribution system," *IEEE Trans. on Power Electron*., vol. 17, no. 3, pp. 438-447, May 2002.